Trafficking and Subcellular Localization of Multiwalled Carbon Nanotubes in Plant Cells

Maged F. Serag,[†,‡,*] Noritada Kaji,[†,‡] Claire Gaillard,[§] Yukihiro Okamoto,[†,‡] Kazuyoshi Terasaka,[⊥] Mohammad Jabasini,[†] Manabu Tokeshi,[†,‡] Hajime Mizukami,[⊥] Alberto Bianco,[§,*] and Yoshinobu Baba[†,‡,¶]

[†]Department of Applied Chemistry, Graduate School of Engineering, [‡]FIRST Research Center for Innovative Nanobiodevice, Nagoya University, Japan, [§]Centre National de la Recherche Scientifique, Institut de Biologie Moléculaire et Cellulaire, UPR 9021 Immunologie et Chimie Thérapeutiques, Strasbourg, France, [⊥]Department of Pharmacognosy, Graduate School of pharmaceutical Sciences, Nagoya City University, Japan, and [¶]National Institute of Advanced Industrial Science and Technology (AIST), Takamatsu, Japan

ABSTRACT Major barriers to delivery of biomolecules are crossing the cellular membranes and achieving a high cytoplasmic concentration by circumventing entrapment into endosomes and other lytic organelles. Motivated by such aim, we have investigated the capability of multiwalled carbon nanotubes (MWCNTs) to penetrate the cell membrane of plant protoplasts (plant cells made devoid of their cell walls *via* enzymatic treatment) and studied their internalization mechanism *via* confocal imaging and TEM techniques. Our results indentified an endosome-escaping uptake mode of MWCNTs by plant protoplasts. Moreover, short MWCNTs (<100 nm) were observed to target specific cellular substructures including the nucleus, plastids, and vacuoles. These findings are expected to have a significant impact on plant cell biology and transformation technologies.

KEYWORDS: carbon nanotubes · functionalization · plant cell · catharanthus protoplasts · endosome escaping · organelle targeting

Owing to their extraordinary physical, chemical, and mechanical properties, carbon nanotubes (CNTs) have been proven to be a useful tool in the field of biomolecular delivery. Single-walled and multiwalled carbon nanotubes (SWCNTs and MWCNTs) have shown a unique ability to host a wide variety of biomolecules and traffic through different cellular barriers.[1−7] An increasing number of studies have reported the toxicological impact and safety profile of carbon nanomaterials on both plant[8] and mammalian cells,[9−12] indicating that a high degree of CNT functionalization leads to a dramatic reduction in toxic effects.[13] Recently, SWCNTs have been shown to have a marked ability to penetrate the cell wall and cell membrane of plant cells while displaying little toxicity. Alternatively, MWCNTs have been found to penetrate tomato seeds and to increase their germination and growth rates with no signs of toxicity.[15] However, to date the majority of CNT cell uptake investigations have focused on mammalian and bacterial cells. Whether MWCNTs can traffic through a plant cell membrane has not been addressed nor has their subcellular distribution.

The plant cell wall is a unique cellular barrier that surrounds plant cells. The most characteristic component of plant cell walls is cellulose, which largely determines their architecture. Together with hemicelluloses and pectin, such thick cellulosic barriers impede the passage of macromolecules into the cell. Therefore plant protoplasts have previously been used to study the internalization of other nanomaterials such as mesoporous silica nanoparticles,[16] quantum dots, and polystyrene nanospheres.[17]

CNT uptake studies are essential for the development of nanotransporters for plant cells, which in turn has a particular importance for plant cell transformation. In addition, understanding the subcellular locations of CNTs is of utmost importance for a possible use of CNTs in intracellular labeling and imaging and for the development of intracellular biosensors leading to the advancement of plant cell biology studies. Herein, we evaluate the ability of functionalized MWCNTs to traffic through protoplast membranes, elucidate their internalization mechanism, and report our ultrastructural observations of their subcellular distribution.

RESULTS AND DISCUSSION

Uptake of CNTs by Plant Protoplasts. MWCNTs labeled with fluorescein isothiocynate (FITC) (hereafter abbreviated MW-F) were prepared and characterized as previously reported.[18] Briefly, MWCNTs were shortened to a range of lengths mainly between

*Address correspondence to a.bianco@ibmc-cnrs.unistra.fr, magedserag@yahoo.com.

Received for review September 8, 2010 and accepted November 24, 2010.

Published online December 8, 2010. 10.1021/nn102344t

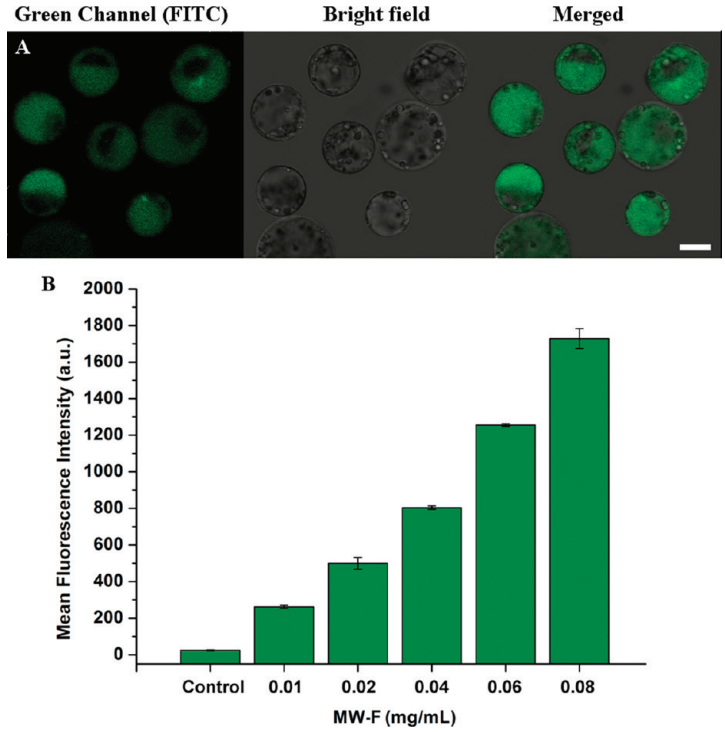

Figure 1. Uptake of MW-F by *C. roseus* protoplasts. (A) Confocal microscopy images of *C. roseus* protoplasts incubated with MW-F (confocal aperture was opened to collect fluorescence from the entire depth of the cells; $Z = 40$ μm). Scale bar: 20 μm. (B) Mean fluorescence intensity of protoplasts incubated with different concentrations of MW-F.

50 and 500 nm, using strong acid conditions.[18] Oxidized MWCNTs underwent the 1,3-dipolar cycloaddition reaction. The ammonium groups introduced around the surface of the nanotubes were subsequently functionalized with FITC.[18]

To prove that MW-F can penetrate the plant cell membrane, we used *Catharanthus roseus* protoplasts (an important medicinal species belonging to Apocynaceae and a difficult-to-transform plant model).[19] *C. roseus* protoplasts suspended in protoplast digest/wash medium (D/W) were incubated for 3 h with MW-F. After being washed with D/W, the cells were imaged by confocal microscopy. Under our experimental conditions, almost all of the cells showed a fluorescence signal attributed to MW-F uptake (Figure 1A). We then varied the concentration of MW-F and observed an increase in cellular fluorescence upon increasing MW-F concentration (Figure 1B). Since cell wall removal renders protoplasts weak and fragile, we only analyzed protoplasts with intact membranes, whereas collapsed cells or cells of abnormal morphology (not exceeding 20% of total protoplast count) marked by an intense fluorescence were excluded during the analysis. In our experiments, the 3 h incubation period, followed by three successive washings with D/W, was sufficient to obtain detectable cell fluorescence while maintaining viability of the protoplasts.

Confocal Investigation of CNT Uptake Mode. We then studied the mechanism of MW-F internalization by *C. roseus* protoplasts. To test whether MW-F is internalized *via* the endosomal pathway, the endosomal membrane was labeled using FM4-64 dye. FM4-64 is a styryl dye with amphiphilic nature, so it only fluoresces in the exoplasmic face of the plasma membrane and does not freely move from the exoplasmic to the cytoplasmic face. As a consequence, FM4-64 is regarded as a robust marker for endocytosis. FM4-64 dye exclusively labels the plasma membrane and then the endosomal membrane structures where it remains trapped in the organelles of the endocytic pathway.[20] Interestingly, only a few endosomes showed enclosure of fluorescent MW-F aggregates (Figure 2A). These endosomes were large-sized and could be distinguished from small endosomes and other organelles of the endocytic pathway. These small structures were responsible for the cytoplasmic background fluorescence of FM4-64 (Figure 2A,B). Co-localization studies of cell areas containing such small structures revealed a poor colocalization between FITC and FM4-64 signals in many confocal 3D-reconstructed images (Figure 2B,C). This suggested that MW-F internalization was poorly associated with the endosmal route. Moreover, blocking the endosomal route *via* incubation of *C. roseus* protoplasts at 4 °C[21] did not have much impact on fluorescence intensity of the protoplasts when compared with the control (Figure S1 in Supporting Information). This concludes that MW-F passively pass through the cell membrane without entrapment into the degrading endosomal organelles and hence become ready to exert their action.

In previous studies, the uptake of FITC by plant protoplasts has been reported to occur *via* both passive diffusion and endosomal route within 20 min. However, the uptake of dextran-FITC occurred exclusively following endosomal route after 18 h of incubation. This delay in dextran-FITC uptake was attributed to inhibition of endocytosis by osmotic stress exerted by dextran.[22,23] Inspired by these studies, we evaluated the internalization of FM4-64 dyes in the presence of varying concentrations of MW-F. After a 2 h incubation period with MW-F, FM4-64 marker was added and protoplasts were further incubated for 1 h. Interestingly, a decrease in the cytoplasmic FM4-64 fluorescence was observed upon increasing the MW-F concentration (Figure 2D). The phenomenon of endocytosis inhibition becomes evident at MW-F concentration of 0.04 mg/mL (Figure 2D). This represents the starting concentration to exploit this phenomenon. In a control experiment and

within 6 h, *C. roseus* cells actively accumulated FITC about 2.5 times more than cells incubated in 0.04 mg/mL MW-F (Figure S2 in Supporting Information) in a similar way as reported for FITC alone and FITC−dextran conjugate.[22] Since increasing MW-F concentration should result in a concomitant increase in medium tonicity, such results clearly demonstrated a tonicity-dependent inhibition of endocytosis by MW-F.

TEM Investigation of CNT Uptake Mode. The confocal microscope only detects gross fluorescence that is emitted from cells. Highly dispersed CNTs, such as single nanotubes, might not be detectable by this technique. Therefore, the cell uptake of single nanotubes should be investigated by other methods, including TEM. Cells incubated with MW-F for 3 h were then observed by TEM. Many images were acquired for the protoplast substructures, and some representative images are shown in Figures 3 and 4 and Supporting Information Figures S3−S12. The cell internalization of isolated MW-F was observed by TEM. For example, Figure 3A and Figure S3A show that a single MW-F was penetrating the cell membrane and tonoplast (vacuolar membrane), respectively. Moreover, most of the examined endosomes did not contain MW-F aggregates (Figure 3B) consistent with confocal microscopy data. Therefore, we observed the isolated MW-F inside cells (Figure 3C,D and Figure S4) as a result of a direct penetration of the plasma membrane, while bundles or aggregates were only observed outside the cells (Figure S5).

Localization of CNT Outside the Endosomal Organelles. Compared to animal systems, plant cell endocytosis is less understood and the tools for studying the mechanisms are limited to membrane-impermeable dyes.[24] On the basis of TEM investigations, endocytosis is believed to start with the formation of endosomes in the endoplasmic face of cell membrane. Endosomes are highly dynamic organelles involved in sorting membrane proteins and extracellular macromolecules through delivery to multivesicular bodies (MVBs) and then to the lytic vacuoles.[25] In the plant cell, the vacuoles occupy most of the cell volume and one of their important functions is molecular degradation and storage. The acidic nature of plant cell vacuoles provides an appropriate environment for carrying out the activities of lysosomal acid hydrolases including nucleases, proteases, and glycosidases.[26] Additionally, in plant protoplasts, where the secretory activity is higher than in the walled cells because of the intense regeneration of the cell wall, endocytosis is directed toward recycling. The endocytosed materials are transferred to the partially coated reticulum (PCR), and then are delivered to the Golgi apparatus which recycles them again toward the plasma membrane.[25] Under our experimental conditions and after careful examination, we could not find MW-F in any organelles associated with the endocytosis cycle. Endosomes, MVBs, and PCR appeared intact (Figure 3B,E and Supporting Information, Figure S6), occasionally contained isolated MW-F (Figure 3F,G), possibly due to direct penetration from the cytoplasm, or very rarely enclosed aggregates of MW-F inside the large endosomes (Figure 2H and the confocal image in Figure 2A). Taken together, our TEM results clearly demonstrated an inhibition of the endocytosis cycle by MW-F. It is important to underline that sometimes CNTs have the tendency to aggregate in solution. On the basis of this phenomenon, our present findings, and findings of previous studies,[22,23] we propose that MW-F nanoaggregates cannot penetrate the plasma mem-

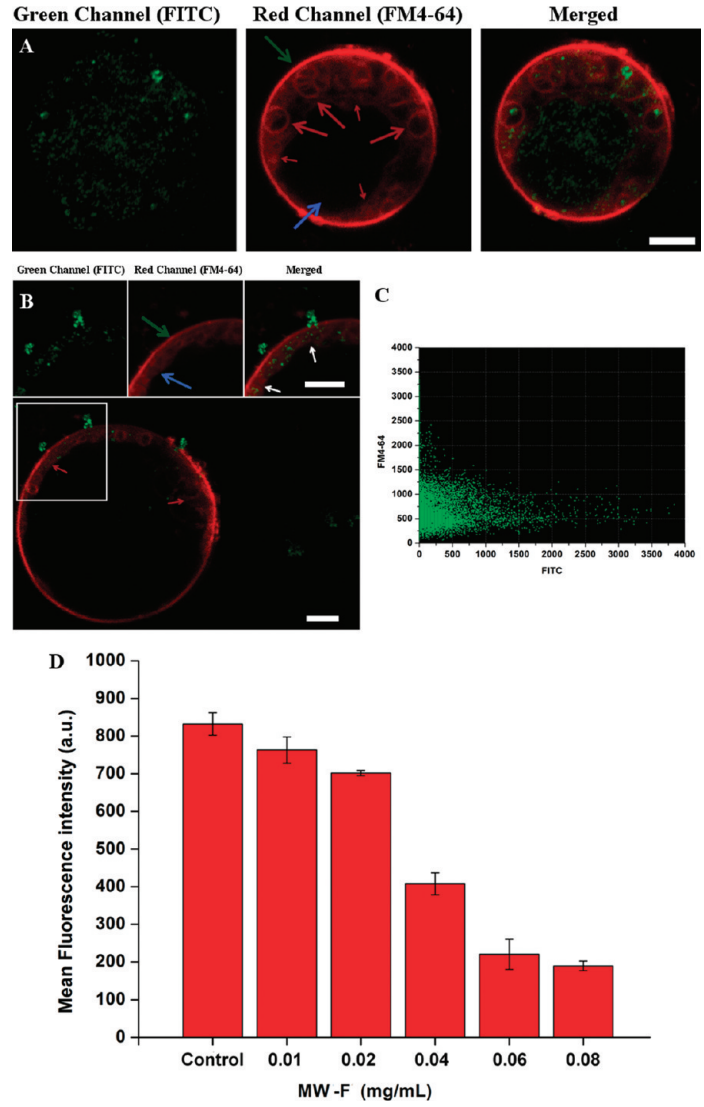

Figure 2. Endosomal uptake of FM4-64 marker by *C. roseus* protoplasts in the presence of MW-F. (A) A protoplast showing accumulation of MW-F (single focal plane; thickness, $Z = 1$ μm). Protoplasts were incubated with MW-F and FM4-64 for 1 h. The green arrow indicates the cell membrane; the blue arrow indicates the vacuole. Long red arrows indicate the large endosomes. Short red arrows indicate the background fluorescence of the small endosomal structures. Scale bars: 5 μm. (B) Another protoplast showing MW-F accumulation. Inset: Three-dimensional reconstructed image of the cell area marked by the white square. The green arrow indicates the cell membrane. The blue arrow indicates the background fluorescence of the small endosomal structures. Scale bar: 5 μm. (C) Colocalization of FITC and FM4-64 signals in the cell area between white arrows in inset of Figure 2B. (D) Mean fluorescence intensity of FM4-64 challenged protoplasts in the presence of different MW-F concentrations.

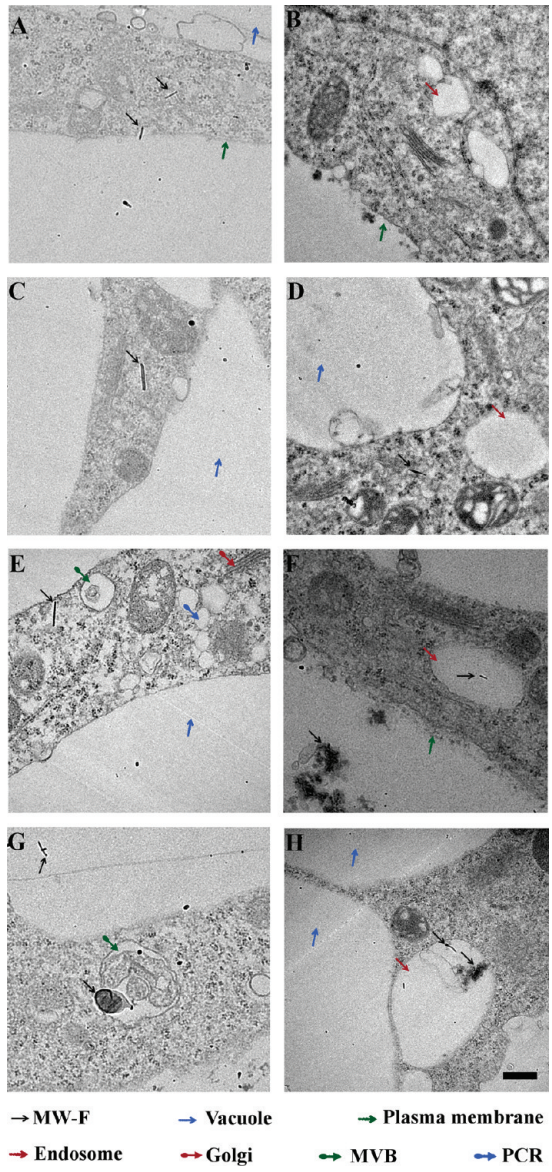

Figure 3. TEM characterization of cell uptake of MW-F. *C. roseus* protoplasts were incubated with MW-F (0.06 mg/mL) at 25 °C for 3 h. (A−D) Localization of MW-F in the cytoplasm. (E−H) Characterization of the organelles of the endosomal pathway. The arrows indicate the cell structures or MW-F. Scale bar: 500 nm. A zoomed-in view of the endosomal area of panel H is illustrated in Supporting Information, Figure S7.

brane and therefore increase the tonicity of the surrounding protoplasts medium. Such tonicity should preclude a fast rate of endocytosis. Meanwhile, MW-F can miss the endosomal cycle and diffuse into the cytoplasm *via* direct penetration. The direct penetration mode is indeed advantageous for biomolecular delivery because it avoids the drawbacks of endocytosis such as endocytic degradation and targeting inefficiency. Of note, other investigations of nanomaterials uptake by plant cells have identified endocytosis as the main mechanism of entry. For example, quantum dots[17] and SWCNTs[14] were rapidly endocytosed into walled plant cells within 2 h, while silica nanoparticles[16] and polystyrene nanospheres[17] were endocytosed by protoplasts.

Subcellular Distribution of CNTs. Because of the direct penetration into cells, single MW-F were frequently observed in the cytoplasm (Figure 3C−E and Supporting Information, Figure S4). The accumulation of isolated MW-F increased their chance to enter different subcellular structures. Although single MW-F could be seen inside many organelles, three main compartments were identified as target sites (*i.e.*, cell vacuole, plastids, and the nucleus). MW-F of different lengths have been identified inside the vacuoles with some of them appearing in sectional views (Figure 4A, Figures S3B−D, S8). The plastids, the sites for photosynthesis and starch accumulation, were also penetrated by MW-F (Figure 4B, Figure S9). The cell nucleus consists of a double layered-membrane that encloses important genetic information about the cell. This membrane is impermeable to most molecules except those that are able to penetrate through nuclear pores.[27] TEM examination identified MW-F inside the nucleus; some of them were observed to have deeply penetrated the nucleus and to be localized in the perinucleolar region (Figure 4C, Figures S10 and S11). These results documented the first direct observation of MWCNTs located in important organelles such as the nucleus and plastids of plant cell.

Preferential Uptake and Distribution of CNTs. We next measured the lengths of individual nanotubes that were taken up by cells after 3 h. Approximately 100 nanotubes with proper orientations were measured and the histogram was generated (Figure 5A). The average lengths of MW-F in cells were around 100 nm. We exam-

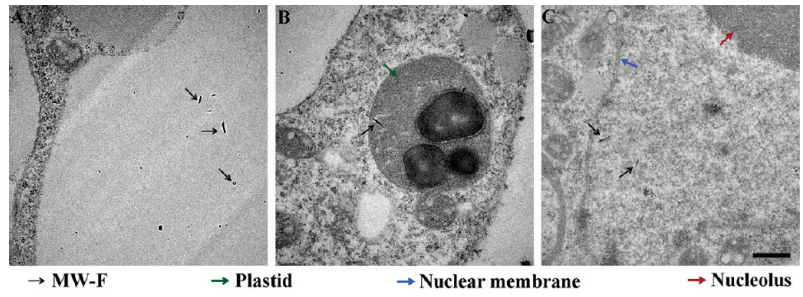

Figure 4. TEM characterization of cellular distribution of MW-F. *C. roseus* protoplasts were incubated with MW-F (0.06 mg/mL) at 25 °C for 3 h. A. Localization of MW-F inside the cell vacuole (black arrows). B. Localization of MW-F inside the plastids. The rounded dark structures represent the starch granules. C. Localization of MW-F inside the cell nucleus. The arrows indicate the cell structures or MW-F. Scale bar: 500 nm.

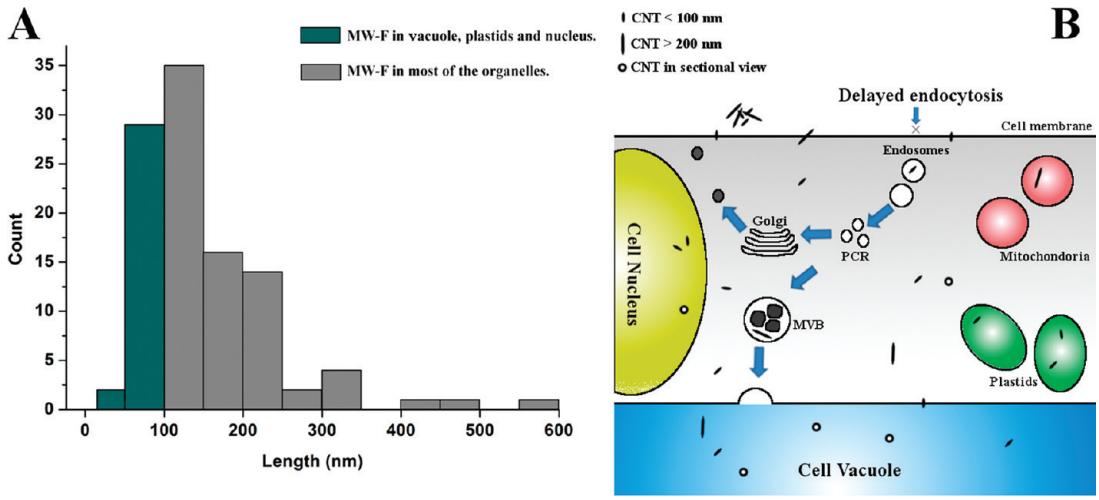

Figure 5. Distribution of MW-F in *C. roseus* protoplasts. (A) Length distribution of MW-F inside protoplasts after 3 h incubation at 25 °C. The histogram was generated based on counting approximately 100 individual MW-F with proper orientations. (B) A model for cell uptake and distribution of MW-F in *C. roseus* protoplasts. The presence of MW-F nanoaggregates increases tonicity of the cell medium. The cell responds by delaying the endocytosis cycle giving a chance for individual nanotubes of varying lengths to penetrate the cell membrane and to miss the endosomal cycle. Individual tubes located in endosomal structures are attributed to direct penetration of their membranes. MW-*F* < 100 nm are localized predominantly in the nucleus, plastids, and vacuoles while longer MW-F can be found in all cell organelles.

ined ~60 TEM micrographs from random transverse sections of 3 independent protoplast cultures treated with MW-F and then only counted those tubes with appropriate orientations while oblique and rounded particles were excluded. The nanotube length distribution therefore represented the best approximation on the basis of our TEM results. The data demonstrated that shorter MW-F had a stronger ability to penetrate protoplast plasma membranes. Through our careful examination of TEM micrographs, we noticed a size-dependent distribution of short MW-F inside organelles. While, long MW-F (>200 nm) were observed inside most subcellular structures, short MW-F (30−100 nm) were only observed inside vacuoles, nucleus, and plastids. Other organelles such as endoplasmic reticulum and mitochondria were observed either intact or penetrated by longer MW-F (Supporting Information, Figure S12). These findings indicated that tonoplast (vacuolar membrane), nuclear membrane, and plastid membrane were penetrable by MW-F within the aforementioned size limit of about 30−100 nm, while the membranes of other organelles seem to hamper the passage of short MW-F. We thought that the physical insertion and diffusion were the most plausible penetration mechanisms of longer MW-F. This differential penetrability of short MW-F offer us an essential strategy for targeting cytoplasm, plastids, and nuclei of plant cells using MWCNTs as a delivery vehicle. Figure 5B illustrates the endosomal cycle as well as the distribution of individual MW-F of different lengths in various cell organelles. Although MW-F occupied many subcelluar organelles, concentrations as high as 0.06 mg/mL showed very little toxicity (Supporting Information, Figure S13).

CONCLUSION

We have studied, for the first time, the capacity of MWCNTs to traverse across a plant cell membrane *via* a direct penetration mechanism rather than endocytosis. In plants, endosomal and recycling pathways often result in degradation and a decrease of the cytoplasmic concentration of the endocytosed materials. Accordingly, missing the plant endocytosis cycle is of particular importance for delivery of biomolecules. The direct penetration mode associated with the especially slow endocytosis rate in a nanotube medium induces MWCNT to escape from endosomes. This phenomenon holds a great promise in designing endosomes-escaping nanotransporters for plant cells based on MWCNTs. Moreover, we observed a size dependent translocation of MWCNTs into important cellular structures including the nucleus and plastids. This can be used effectively to deliver molecular cargos into specific compartments; this is a property that we expect to have a significant impact on both plant cell biology and transformation technologies. The study of the internalization and distribution mechanism of CNTs in plant cells, and the exploration of further novel behaviors deserve further studies.

EXPERIMENTAL SECTION

Carbon Nanotubes. >Purified multiwalled carbon nanotubes (MWCNTs) were purchased from Nanostructured & Amorphous Materials Inc. (Houston, TX). Regular MWCNTs used in this study were 95% pure, stock no. 1240XH. Outer average diameter was between 20 and 30 nm, and length between 0.5 and 2 μm before oxidative treatment. The oxidation and functionalization of the nanotubes with the fluorescent

probe (FITC) were performed as described by Gaillard *et al*.[18]

Plant Material. *Catharanthus roseus* cell suspension culture was initiated in Murashig and Skoog medium with minimal organics (MSMO, Sigma, St. Louis, MO) supplemented with 1 μM 2,4-diphenoxy acetic acid and 1 μM kinetin. Culture flasks were put in a shaker operated at 130 rpm and incubated at 25 °C in dark. After 4 days of cultivation, the cells were used for protoplasts isolation.

Protoplast Isolation. All chemicals were purchased from Sigma (St. Louis, MO). All steps were carried out under aseptic conditions. Suspension cultured *C. roseus* cells were separated from the growth medium by filtration and were washed twice in fresh MSMO medium. Cells were resuspended in protoplast digest/wash solution (D/W) containing 4% (W/V) Cellulase. A 50 mL portion of the resuspended culture was poured in into 100 mL flask, and the flask was placed in a shaker operated at 100 rpm at room temperature for 4 h. Protoplasts were separated from intact cells by passing them through a cell strainer (BD Falcon; 70 μm Nylon) and then centrifuged at 1000 rpm for 5 min. The protoplast pellet was washed three times with D/W medium.

Incubation of Protoplasts with MW-F. A 0.5 mL portion of protoplast suspension (50000 cell/mL) in D/W medium was transferred to a 4-well LabTek chamber. A 100 μL portion of MW-F at different concentrations was added to the protoplast suspension, and then the cells were incubated in the dark at either 25 or 4 °C for 3 h. After incubation, the cells were washed three times with D/W, and then resuspended in D/W for confocal imaging or TEM observations.

Confocal Microscopy Imaging of Plant Cells. A 300 μL aliquot of protoplast suspension was placed in glass bottom dishes (Matsunami, JAPAN). Protoplasts live cell images were taken using 10× and 40× objectives lenses on a laser scanning confocal microscope (Olympus, FV1000) equipped with a multiline Ar laser (458, 488, 515 nm), a HeNe(G) laser (543 nm, 1 mW) and an AOTF laser combiner plus a set of ion deposition and barrier filters. Images were acquired and analyzed using Fluoview software. To calculate the mean fluorescence intensity, the fluorescence intensities of cells (about 300 protoplasts) were averaged.

Protoplast Staining with FM4-64 Dye. FM4-64 dye (Invitrogen, Molecular Probe) was dissolved in cold phosphate buffer (pH = 7) at a concentration of 5 μg/mL; 10 μL of FM4-64 was added to 300 μL of protoplast suspension with MW-F and then incubated for 1 h unless otherwise stated.

Protoplast Viability Testing. Protoplasts viability was evaluated using plant cell viability assay kit (Sigma, St. Louis, MO) following the accompanying protocol.

Transmission Electron Microscopy. *C. roseus* protoplasts were treated with 0.4 mg/mL MW-F for 3 h. The protoplasts were then fixed in 4% glutaraldehyde in D/W medium for 1 h at room temperature and then in a refrigerator overnight. After rinsing with 0.05 M potassium phosphate buffer (pH 7.0), the cells were postfixed in 2% osmium tetroxide for 1 h. They were then dehydrated through a graded series of acetone and embedded in Spurr's resin. Ultrathin sections (approximately 90 nm in thickness) were cut with a diamond knife on an ultramicrotome (Leica ultracut S). After the sections were stained with uranyl acetate and lead citrate, they were observed in a JEOL JEM 2100F TEM at an accelerating voltage of 200 kV. Images were taken on a Gatan 1 k × 1 k CCD Camera.

Acknowledgment. We are grateful to Drs. Koji Nitta and Atsushi Kitayama, Terabase Inc., and Prof. Kuniaki Nagayama, Okazaki Institute for Integrative Bioscience, National Institutes of Natural Sciences, for the TEM observations. This research was partly supported by Industrial Technology Research Grant Program in 2009 from New Energy and Industrial Technology Development Organization (NEDO) of Japan and the Japan Society for the Promotion of Science (JSPS) through its "Funding Program for World-Leading Innovative R&D on Science and Technology (FIRST Program). This work was supported by the "Centre National de la Recherche Scientifique". C.G. is grateful to the European Union, NEURONANO program (NMP4-CT-2006-031847) for financing her Ph.D.

Supporting Information Available: Control experiments, additional TEM micrographs and cytotoxicity results. This material is available free of charge *via* the Internet at http://pubs.acs.org.

REFERENCES AND NOTES

1. Cai, D.; Mataraza, J.; Qin, Z.; Huang, Z.; Huang, J.; Chiles, T.; Carnagan, D.; Kempa, K.; Ren, Z. Highly Efficient Molecular Delivery into Mammalian Cells Using Carbon Nanotube Spearing. *Nat. Methods* **2005**, *2*, 449–454.
2. Kostareleos, K.; Lacerda, L.; Pastorin, G.; Wu, W.; Sébastien, W.; Jacqueline, L.; Godefroy, S.; Pantarotto, D.; Briand, J. P.; Muller, S.; *et al*. A. Cellular Uptake of Functionalized Carbon Nanotubes Is Independent of Functional Group and Cell Type. *Nat. Nanotechnol.* **2007**, *2*, 108–113.
3. Gao, L.; Nie, L.; Wang, T.; Qin, Y.; Guo, Z.; Yang, D.; Yan, X. Carbon Nanotube Delivery of the GFP Gene into Mammalian Cells. *Chembiochem* **2006**, *7*, 239–242.
4. Pantarotto, D.; Briand, J. P.; Prato, M.; Bianco, A. Translocation of Bioactive Peptides across Cell Membranes by Carbon Nanotubes. *Chem. Commun.* **2004**, *43*, 5242–5246.
5. Shi Kam, N. W.; Dai, H. Carbon Nanotubes as Intracellular Protein Transporters: Generality and Biological Functionality. *J. Am. Chem. Soc.* **2005**, *127*, 6021–6026.
6. Shi Kam, N. W.; O'Connell, M.; Wisdom, J. A.; Dai, H. Carbon Nanotubes as Multifunctional Biological Transporters and Near-Infrared Agents for Selective Cancer Cell Destruction. *Proc. Natl. Acad. Sci. U.S.A.* **2005**, *102*, 11600–11605.
7. Bianco, A.; Kostarelos, K.; Partidos, C. D.; Prato, M. Application of Carbon Nanotubes in Drug Delivery. *Curr. Opin. Chem. Biol.* **2005**, *9*, 674–679.
8. Lin, D.; Xing, B. Phytotoxicity of Nanoparticles: Inhibition of Seed Germination and Root Growth. *Environ. Pollut.* **2007**, *150*, 243–250.
9. Sato, Y.; Yokoyama, A.; Shibata, K.; Akimoto, Y.; Ogino, S.; Nodasaka, Y.; Kohgo, T.; Tamura, K.; Akasaka, T.; Uo, M.; *et al*. Influence of Length on Cytotoxicity of Multi-Walled Carbon Nanotubes against Human Acute Monocytic Leukemia Cell Line THP-1 *in Vitro* and Subcutaneous Tissues of Rats *in Vivo*. *Mol. Biosyst.* **2005**, *1*, 176–182.
10. Kagan, V. E.; Tyurina, Y. Y.; Tyurin, V. A.; Konduru, N. V.; Potapovich, A. I.; Osipov, A. N.; Kisin, E. R.; Schwegler-Berry, D.; Mercer, R.; Castranova, V; *et al*. Direct and Indirect Effect of Single-Walled Carbon Nanotubes on RAW 264.7 Macrophages: Role of Iron. *Toxicol. Lett.* **2006**, *165*, 88–100.
11. Pulskamp, K.; Diabaté, S.; Krug, H. F. Carbon Nanotubes Show No Sign of Acute Toxicity but Induce Intracellular Reactive Oxygen Species in Dependence on Contaminants. *Toxicol. Lett.* **2006**, *168*, 58–74.
12. Dumortier, H.; Lacotte, S.; Pastorin, G.; Marega, R.; Wu, W.; Bonifazi, D.; Briand, J. P.; Prato, M.; Muller, S.; Bianco, A. Functionalized Carbon Nanotubes Are Noncytotoxic and Preserve the Functionality of Primary Immune Cells. *Nano Lett.* **2006**, *6*, 1522–1528.
13. Sayes, C. M.; Liang, F.; Hudson, J. L.; Mendez, J.; Guo, W.; Beach, J. M.; Moore, V. C.; Doyle, C. D.; West, J. L.; Billups, W. E.; *et al*. Functionalization Density Dependence of Single-Walled Carbon Nanotubes Cytotoxicity *in Vitro*. *Toxicol. Lett.* **2006**, *161*, 135–142.
14. Liu, Q.; Chen, B.; Wang, Q.; Shi, X.; Xiao, Z.; Lin, J.; Fang, X. Carbon Nanotubes as Molecular Transporters for Walled Plant Cells. *Nano Lett.* **2009**, *9*, 1007–1010.
15. Khodakovskaya, M.; Dervishi, E.; Mahmood, M.; Xu, Y.; Li, Z.; Watanabe, F.; Biris, A. Carbon Nanotubes Are Able To Penetrate Plant Seed Coat and Dramatically Affect Seed Germination and Plant Growth. *ACS Nano* **2009**, *3*, 3221–3227.
16. Torney, F.; Trewyn, B. G.; Lin, V. S. -Y.; Wang, K. Mesoporous Silica Nanoparticles Deliver DNA and Chemicals into Plants. *Nat. Nanotechnol.* **2007**, *2*, 295–300.
17. Etxeberria, E.; Gonzalez, P.; Baroja-Fernandez, E.; Pozueta-Romero, J. Fluid Phase Uptake of Artificial Nano-spheres and Fluorescent Quantum-Dots by Sycamore Cultured Cells. *Plant Signaling Behav.* **2006**, *1*, 196–200.

18. Gaillard, C.; Cellot, G.; Li, S.; Toma, F. M.; Dumortier, H.; Spalluto, G.; Cacciari, B.; Prato, M.; Ballerini, L.; Bianco, A. Carbon Nanotubes Carrying Cell-Adhesion Peptides Do Not Interfere With Neuronal Functionality. *Adv. Mater.* **2009**, *21*, 2903–2908.
19. Our unpublished results and personal communication from other collaborating groups.
20. Griffing, L. FRET Analysis of Transmembrane Flipping of FM4-64 in Plant Cells: Is FM4-64 a Robust Marker for Endocytosis. *J. Micorosc.* **2008**, *231*, 291–298.
21. Emans, N.; Zimmermann, S.; Fisher, R. Uptake of a Fluorescent Marker in Plant Cells Is Sensitive to Brefeldin A and Wortamannin. *Plant Cell* **2002**, *14*, 71–86.
22. Cole, L.; Coleman, J.; Evans, D.; Hawes, C. Internalization of Fluorescein Isothiocyanate and Fluorescein Isothiocyanate-Dextran by Suspension-Cultured Plant Cells. *J. Cell Sci.* **1990**, *96*, 721–730.
23. Bahaji, A.; Aniento, F.; Cornejo, M. Uptake of an Endocytic Marker by Rice Cells: Variations Related to Osmotic and Saline Stress. *Plant Cell Physiol.* **2003**, *44*, 1100–1111.
24. Šamaj, J. *Methods and Molecular Tools for Studying Endocytosis in Plants: An Overview in Plant Endocytosis*; Šamaj, J., Baluška, F., Menzel, D., Eds.; Springer: Berlin, 2006; pp 1−17.
25. Low, S. P.; Chandra, S. Endocytosis in Plants. *Annu. Rev. Plant Physiol. Plant Mol. Biol.* **1994**, *54*, 609–631.
26. Marty, F. Plant Vacuoles. *Plant Cell* **1999**, *11*, 587–599.
27. Terry, L. J.; Shows, E. B.; Wente, S. R. Crossing the Nuclear Envelope. *Science* **2007**, *318*, 1412–1416.